Quadrupole-dipole Raman scattering at the 1S yellow exciton in Cu_2O†

A. Z. Genack and H. Z. Cummins*
Department of Physics, City College of The City University of New York, New York, New York 10031

M. A. Washington‡
Department of Physics, New York University, New York, New York 10003

A. Compaan
Department of Physics, Kansas State University, Manhattan, Kansas 66506
(Received 21 April 1975)

Normally forbidden Raman scattering is observed from the seven odd-parity phonons of Cu_2O with the exciting laser in resonance with the quadrupole 1S yellow exciton. Polarization ratios are obtained in a number of scattering geometries and shown to be consistent with the third-rank tensor derived by Birman for Raman scattering mediated by quadrupole-dipole states. Enhanced scattering is observed from the LO components of the two polar modes which we attribute to the dipole term in the expansion of the Fröhlich intraband exciton-lattice interaction. From a comparison of the intensities of Raman scattering from the LO and TO components of both polar modes the contributions of the Fröhlich and deformation-potential interactions to the observed Raman scattering are estimated. Finally the symmetry of the Raman tensor for time-reversed processes and the relationship of scattering at an "in" resonance to that at an "out" resonance is demonstrated.

I. INTRODUCTION

Compaan and Cummins[1] have recently observed Raman scattering from all the odd-parity phonons of Cu_2O when the incident laser frequency is in resonance with the 1S yellow (1SY) exciton of quadrupole symmetry Γ_{25}^+.[2] This scattering is forbidden in the usual Raman mechanism which involves dipole-allowed exciton states and even-parity phonons. A new mechanism for Raman scattering, involving virtual electric-quadrupole- and electric-dipole states was proposed to explain the anomalous scattering.[1] Birman[3] has subsequently derived the scattering tensors for the electric-quadrupole–electric-dipole (EQ-ED) Raman mechanism. These tensors predict a completely new set of polarization-selection rules for Raman scattering at dipole-forbidden states. We have confirmed these selection rules and thereby verfied that first-order Raman scattering at the 1SY exciton is due to the EQ-ED mechanism. The results of our polarization study of Raman scattering at the 1SY exciton are presented in Sec. II of this paper.

The intensity of first-order Raman scattering by phonons is given in third-order pertubation theory[4] by

$$I(\omega_i, \omega_s, \omega_0) \sim \left| \sum_{a,b} \frac{\langle f|\mathcal{H}_{ER}|a\rangle\langle a|\mathcal{H}_{EL}|b\rangle\langle b|\mathcal{H}_{ER}|i\rangle}{(\omega_s-\omega_a)(\omega_i-\omega_b)} + T \right|^2, \tag{1}$$

where ω_i, ω_s, and ω_0 are the incident, scattered, and phonon frequencies with $\omega_i = \omega_s + \omega_0$ for a Stokes process; $|i\rangle$, $|f\rangle$ are the initial and final states, and $|a\rangle$, $|b\rangle$ are intermediate states whose electronic components have complex energies $\hbar\omega_a$ and $\hbar\omega_b$, and T means all time orders. For an "in" resonance with the 1SY exciton, with which we will be primarily concerned, $\omega_i - \omega_b = i\Gamma_{1SY}$ where $\Gamma_{1SY} = 0.4\ \mathrm{cm}^{-1}$ is the energy width of the exciton.[1,5] Similar considerations apply to an "out" resonance where $\omega_s - \omega_a = i\Gamma_{1SY}$. Only the physical time ordering written out explicitly in Eq. (1) contributes significantly to the Raman amplitude at resonance.

The leading term in the expansion for the radiation field which couples to the dipole forbidden 1SY exciton is the electric-quadrupole term, giving the matrix element

$$\langle b|\mathcal{H}_{ER}|i\rangle \sim iA_0\langle b|\vec{k}_i\cdot\vec{r}\,\hat{\epsilon}\cdot\vec{p}|i\rangle. \tag{2}$$

where A_0, $\vec{k}_i$, and $\hat{\epsilon}$ are the vector potential, wave vector, and polarization of the incident radiation field, and $\vec{r}$ and $\vec{p}$ are the electron position and momentum operators. The matrix element associated with the scattered photon with polarization $\hat{\epsilon}'$ has the usual dipole form,

$$\langle f|\mathcal{H}_{ER}|a\rangle \sim A_0\langle f|\hat{\epsilon}'\cdot\vec{p}|a\rangle. \tag{3}$$

Though the exciton-radiation matrix element is nonzero only in second order at a quadrupole-exciton state, a large scattered intensity may, nonetheless, be observed at resonance, since the energy width of a dipole-forbidden level may be very narrow.

The Raman intensity may be put into the form[3]

$$I^j = C\sum_\sigma \left| \sum_{\alpha\beta\gamma} \epsilon'_\alpha P_{\alpha\beta\gamma}(j\sigma)\,\epsilon_\beta k_\gamma \right|^2, \tag{4}$$

TABLE I. Scattering tensors $P_{\alpha\beta\gamma}(j\sigma)$ for EQ(Γ_{25}^{+} – ED scattering with the laser frequency in resonance with a Γ_{25}^{+} exciton state in $O_h - m3m$, $\hat{k}_i = \gamma$. This table was reproduced from J. L. Birman, Phys. Rev. B 9, 4518 (1974).

	$\sigma=(1)$	$\sigma=(2)$	$\sigma=(3)$
		Γ^{2-}	
$\gamma=x$;	$\begin{pmatrix} \cdot & \cdot & \cdot \\ \cdot & \cdot & a \\ \cdot & a & \cdot \end{pmatrix}$		
$\gamma=y$;	$\begin{pmatrix} \cdot & \cdot & a \\ \cdot & \cdot & \cdot \\ a & \cdot & \cdot \end{pmatrix}$		
$\gamma=z$;	$\begin{pmatrix} \cdot & a & \cdot \\ a & \cdot & \cdot \\ \cdot & \cdot & \cdot \end{pmatrix}$		
		Γ^{12-}	
$\gamma=x$;	$\begin{pmatrix} \cdot & \cdot & \cdot \\ \cdot & \cdot & -b\sqrt{3} \\ \cdot & \cdot & \cdot \end{pmatrix}$	$\begin{pmatrix} \cdot & \cdot & \cdot \\ \cdot & \cdot & b \\ \cdot & -2b & \cdot \end{pmatrix}$	
$\gamma=y$;	$\begin{pmatrix} \cdot & \cdot & b\sqrt{3} \\ \cdot & \cdot & \cdot \\ \cdot & \cdot & \cdot \end{pmatrix}$	$\begin{pmatrix} \cdot & \cdot & b \\ \cdot & \cdot & \cdot \\ -2b & \cdot & \cdot \end{pmatrix}$	
$\gamma=z$;	$\begin{pmatrix} \cdot & b\sqrt{3} & \cdot \\ -b\sqrt{3} & \cdot & \cdot \\ \cdot & \cdot & \cdot \end{pmatrix}$	$\begin{pmatrix} \cdot & b & \cdot \\ b & \cdot & \cdot \\ \cdot & \cdot & \cdot \end{pmatrix}$	
		Γ^{15-}	
$\gamma=x$;	$\begin{pmatrix} \cdot & \cdot & \cdot \\ \cdot & c & \cdot \\ \cdot & \cdot & c \end{pmatrix}$	$\begin{pmatrix} \cdot & c & \cdot \\ \cdot & \cdot & \cdot \\ \cdot & \cdot & \cdot \end{pmatrix}$	$\begin{pmatrix} \cdot & \cdot & c \\ \cdot & \cdot & \cdot \\ \cdot & \cdot & \cdot \end{pmatrix}$
$\gamma=y$;	$\begin{pmatrix} \cdot & \cdot & \cdot \\ c & \cdot & \cdot \\ \cdot & \cdot & \cdot \end{pmatrix}$	$\begin{pmatrix} c & \cdot & \cdot \\ \cdot & \cdot & \cdot \\ \cdot & \cdot & c \end{pmatrix}$	$\begin{pmatrix} \cdot & \cdot & \cdot \\ \cdot & \cdot & c \\ \cdot & \cdot & \cdot \end{pmatrix}$
$\gamma=z$;	$\begin{pmatrix} \cdot & \cdot & \cdot \\ \cdot & \cdot & \cdot \\ c & \cdot & \cdot \end{pmatrix}$	$\begin{pmatrix} \cdot & \cdot & \cdot \\ \cdot & \cdot & \cdot \\ \cdot & c & \cdot \end{pmatrix}$	$\begin{pmatrix} c & \cdot & \cdot \\ \cdot & c & \cdot \\ \cdot & \cdot & \cdot \end{pmatrix}$
		Γ^{25-}	
$\gamma=x$;	$\begin{pmatrix} \cdot & \cdot & \cdot \\ \cdot & d & \cdot \\ \cdot & \cdot & -d \end{pmatrix}$	$\begin{pmatrix} \cdot & -d & \cdot \\ \cdot & \cdot & \cdot \\ \cdot & \cdot & \cdot \end{pmatrix}$	$\begin{pmatrix} \cdot & \cdot & d \\ \cdot & \cdot & \cdot \\ \cdot & \cdot & \cdot \end{pmatrix}$
$\gamma=y$;	$\begin{pmatrix} \cdot & \cdot & \cdot \\ d & \cdot & \cdot \\ \cdot & \cdot & \cdot \end{pmatrix}$	$\begin{pmatrix} -d & \cdot & \cdot \\ \cdot & \cdot & \cdot \\ \cdot & \cdot & d \end{pmatrix}$	$\begin{pmatrix} \cdot & \cdot & \cdot \\ \cdot & \cdot & -d \\ \cdot & \cdot & \cdot \end{pmatrix}$
$\gamma=z$;	$\begin{pmatrix} \cdot & \cdot & \cdot \\ \cdot & \cdot & \cdot \\ -d & \cdot & \cdot \end{pmatrix}$	$\begin{pmatrix} \cdot & \cdot & \cdot \\ \cdot & \cdot & \cdot \\ \cdot & d & \cdot \end{pmatrix}$	$\begin{pmatrix} d & \cdot & \cdot \\ \cdot & -d & \cdot \\ \cdot & \cdot & \cdot \end{pmatrix}$

where $P_{\alpha\beta\gamma}(j\sigma)$ is a component of the third-rank scattering tensor for a phonon of polarization σ belonging to the jth irreducible representation. In contrast to the second-rank tensor associated with allowed dipole scattering, which has been given, for example, by Loudon,[6,7] the exciton-radiation interaction is not symmetric with respect to the incident and scattered photons. In the multipole-dipole (MD) mechanism, scattering depends upon the wave vector $\vec{k}$ of the photon that couples to a multipole state. For Cu_2O which has O_h symmetry, the operator $(\vec{k}\cdot\vec{r}\,\hat{\epsilon}\cdot\vec{p})$ transforms as $\Gamma_{25}^{+}\oplus\Gamma_{12}^{+}\oplus\Gamma_{15}^{+}$. Phonons that participate in EQ(Γ_{25}^{+})-ED Raman scattering at the 1SY exciton must transform according to a representation contained in $\Gamma_{25}^{+}\otimes\Gamma_{15}^{-}$ $=\Gamma_{25}^{-}\oplus\Gamma_{12}^{-}\oplus\Gamma_{15}^{-}\oplus\Gamma_{2}^{-}$. All these phonons show enhanced scattering when the laser frequency is near the 1SY exciton.

The tensors $P_{\alpha\beta\gamma}(j\sigma)$ for ω_i in resonance with a dipole-forbidden state have 27 components and are represented by Birman[3] in three slices indexed by the Cartesian components of the incident-photon wave vector $\vec{k}_i$. These tensors for EQ(Γ_{25}^{+})-ED scattering are reproduced in Table I. The Raman constants a, b, c, and d in these tensors are reduced matrix elements which contain the microscopic dynamics and determine the scattering amplitude.

To consider scattering from the two polar Γ_{15}^{-} modes, we must compose the longitudinal (LO) and transverse (TO) components by taking appropriate vectorial combination of tensors of polarization components $\sigma = x, y, z$ given in Table I. The LO and TO components are split by the macroscopic electric field $\vec{E}_L$ carried by the LO phonon.[4,8] Scattering tensors for the Γ_{15}^{-} mode are given in Table II for three scattering configurations which we have studied in our experiments. The Raman constant for the LO phonon can be written as $c = c_D + c_F$, where c_D is the Raman constant for the TO phonons, which is related to scattering via the deformation potential, and c_F accounts for the additional coupling via the Fröhlich interaction,[9] which is due to the existence of $\vec{E}_L$. This coupling, which was not included in Birman's discussion,[3] vanishes in crystals with inversion symmetry in ordinary dipole Raman scattering but can exist for EQ-ED scattering.[10] From measurements of the intensity of scattering from the LO and TO components of the two sets of Γ_{15}^{-} modes, we will obtain an estimate for the relative importance of the Fröhlich and deformation-potential interactions for Raman scattering at the 1SY exciton. This will be discussed in Sec. III.

A number of underlying symmetries of the Raman tensor can be conveniently tested at resonance with a quadrupole-exciton level. In Sec. IV the symmetry of the Raman tensor for time-

TABLE II. Scattering tensors $P_{\alpha\beta\gamma}(\Gamma_{15}^{-}\sigma)$ for $EQ(\Gamma_{25}^{+})$ – ED Raman scattering for three scattering geometries. For LO phonons $c = c_D + c_F$, where c_D and c_F are Raman constants for scattering via the deformation potential and Fröhlich interaction, respectively.

σ: LO	σ: TO_1	σ: TO_2
	$x(\hat{\epsilon}, \hat{\epsilon}')y$	
$\sigma = x - y$	$\sigma = x + y$	$\sigma = z$
$\frac{1}{\sqrt{2}}\begin{pmatrix} \cdot & (c_D+c_F) & \cdot \\ \cdot & (c_D+c_F) & \cdot \\ \cdot & \cdot & (c_D+c_F) \end{pmatrix}$	$\frac{1}{\sqrt{2}}\begin{pmatrix} \cdot & -c_D & \cdot \\ \cdot & c_D & \cdot \\ \cdot & \cdot & c_D \end{pmatrix}$	$\begin{pmatrix} \cdot & \cdot & c_D \\ \cdot & \cdot & \cdot \\ \cdot & \cdot & \cdot \end{pmatrix}$
	$x - y(\hat{\epsilon}, \hat{\epsilon}')y - x$	
$\sigma = x - y$	$\sigma = z$	$\sigma = x + y$
$\frac{1}{2}\begin{pmatrix} (c_D+c_F) & -(c_D+c_F) & \cdot \\ -(c_D+c_F) & (c_D+c_F) & \cdot \\ \cdot & \cdot & 2(c_D+c_F) \end{pmatrix}$	$\frac{1}{\sqrt{2}}\begin{pmatrix} \cdot & \cdot & c_D \\ \cdot & \cdot & -c_D \\ \cdot & \cdot & \cdot \end{pmatrix}$	$\frac{1}{2}\begin{pmatrix} -c_D & c_D & \cdot \\ -c_D & c_D & \cdot \\ \cdot & \cdot & \cdot \end{pmatrix}$
	$x + y + z(\hat{\epsilon}, \hat{\epsilon}') - x - y - z$	
$\sigma = x + y + z$	$\sigma = x + y - 2z$	$\sigma = x - y$
$\frac{1}{3}\begin{pmatrix} 2(c_D+c_F) & (c_D+c_F) & (c_D+c_F) \\ (c_D+c_F) & 2(c_D+c_F) & (c_D+c_F) \\ (c_D+c_F) & (c_D+c_F) & 2(c_D+c_F) \end{pmatrix}$	$\frac{1}{3\sqrt{2}}\begin{pmatrix} -c_D & c_D & -2c_D \\ c_D & -c_D & -2c_D \\ c_D & c_D & 2c_D \end{pmatrix}$	$\frac{1}{\sqrt{6}}\begin{pmatrix} -c_D & -c_D & \cdot \\ c_D & c_D & \cdot \\ c_D & -c_D & \cdot \end{pmatrix}$

reversed processes and the relationship of scattering at an "in" resonance to that at an "out" resonance is demonstrated for laser frequencies near the 1SY frequency.

II. TEST OF SELECTION RULES

Raman-scattering experiments were performed at 4 °K on two Cu_2O crystals supplied to us by R. A. Forman of the National Bureau of Standards. The crystals were cut from a large boule grown by Brower and Parker[11] using a floating-zone technique. One crystal was cut along the principal axes and studied using a right-angle scattering geometry. The scattering configuration was $x(\hat{\epsilon}, \hat{\epsilon}')y$, where $\hat{\epsilon}$ and $\hat{\epsilon}'$ refer to the polarizations of the incident and scattered light. Absorption corrections for this configuration were neglibible for our 1-mm-thick crystal at 4 °K at the 1SY exciton frequency. The second crystal was studied in a backscattering geometry with configuration $x - y(\hat{\epsilon}, \hat{\epsilon}')y - x$.

The crystals were mechanically polished and etched with concentrated HNO_3 before being inserted into a helium exchange gas cell in a liquid-helium "Cryo-tip" Dewar.[12] 10 mW of laser power at the 1SY frequency of 16 399 cm^{-1} were obtained from a Spectra Physics model-370 cw dye laser pumped by a Coherent Radiation model-52 argon laser. The dye-laser output was narrowed with an intracavity etalon giving a bandwidth of about 0.06 cm^{-1}.

The results of our polarization study with the laser in resonance with the 1SY exciton are shown in Table III for $x(\hat{\epsilon}, \hat{\epsilon}')y$ scattering and in Table IV for $x - y(\hat{\epsilon}, \hat{\epsilon}')y - x$ scattering. The polarization of the light parallel and perpendicular to the scattering plane is denoted as H and V, respectively. Also shown are the predictions of the $EQ(\Gamma_{25}^{+})$-ED mechanism for these geometries from Table I and II. The observed intensities in each of these Tables are normalized to the average scattering intensity from the phonon of Γ_{25}^{-} symmetry in allowed polarizations. This normalization facilitates comparisons between the tables since the theoretical intensity for scattering from the Γ_{25}^{-} phonon is proportional to d^2 in both geometries in all allowed polarizations.

We have observed the LO-TO splitting of both Γ_{15}^{-} modes, and results for the LO and TO components are listed separately in the tables. This is the first observation of the 2.5-cm^{-1} splitting of the lower-frequency $\Gamma_{15}^{-(1)}$ mode. The TO component of the higher-frequency $\Gamma_{15}^{-(2)}$ mode has previously been observed in Raman scattering, but was probably activated by impurities.[13] In order to resolve the splitting of the $\Gamma_{15}^{-(1)}$ mode, a spectrometer resolution of 0.9 cm^{-1} was used instead of the 1.9-cm^{-1} resolution used for all other lines. The data

TABLE III. Polarization study of Raman scattering with the laser in resonance with 1SY exciton state for scattering in the $x(\hat{\epsilon},\hat{\epsilon}')y$ configuration. Observed intensities are normalized to the signal for the Γ_{25}^- phonon averaged over allowed polarizations (see text for details). Theoretical intensities are given in terms of independent Raman amplitudes, as calculated from Tables I and II.

Phonon	(V,V)	(V,H)	(H,V)	(H,H)
$\Gamma_{25}(88\ \mathrm{cm}^{-1})$				
obs.	0.95	0.98	0.30	1.06
calc.	d^2	d^2	0	d^2
$\Gamma_{12}^-(109\ \mathrm{cm}^{-1})$				
obs.	11.4	15.5	50	11.5
calc.	0	0	$4b^2$	0
$\Gamma_{15}^{-(1)}$(TO: 152 cm^{-1})				
obs.	0.48	0.74	0.13	0.64
calc.	$\frac{1}{2}c_{D_1}^2$	$c_{D_1}^2$	0	$\frac{1}{2}c_{D_1}^2$
$\Gamma_{15}^{-(1)}$(LO: 154.5 cm^{-1})				
obs.	1.05	0.27	0.31	0.78
calc.	$\frac{1}{2}(c_D+c_{F_1})^2$	0	0	$\frac{1}{2}c_{D_1}^2$
$\Gamma_{15}^-(350\ \mathrm{cm}^{-1})$				
obs.	0.04	0.01	0.15	0.01
calc.	0	0	a^2	0
$\Gamma_{15}^{-(2)}$(TO: 635 cm^{-1})				
obs.	0.37	0.28	0.09	0.30
calc.	$\frac{1}{2}c_{D_2}^2$	$c_{D_2}^2$	0	$\frac{1}{2}c_{D_2}^2$
$\Gamma_{15}^{-(2)}$(LO: 665 cm^{-1})				
obs.	1.36	0.46	0.51	1.27
calc.	$\frac{1}{2}(c_{D_2}+c_{F_2})^2$	0	0	$\frac{1}{2}(c_{D_2}+c_{F_2})^2$

recorded in the tables have been scaled to correspond to the spectrometer sensitivity with 1.9-cm^{-1} slits. The LO and TO components of the $\Gamma_{15}^{-(2)}$ mode are broader than the spectrometer resolution, and the integrated intensities of these lines are therefore tabulated.

In Tables III and IV every line shows greatest intensity in the theoretically allowed configurations. We attribute the presence of considerable scattering intensity in forbidden polarizations to the imperfect optical quality of the crystal. X-ray and neutron-diffraction studies show the presence of small-angle (2°–4°) grain boundaries in these crystals, and the laser beam transmitted through the 1-mm-thick crystal showed 10% depolarization. Some additional depolarization results from surface irregularities after etching and from some misalignment of the crystal during mounting. In addition in the backscattering experiments, the incident beam made an angle of 20° with the normal which gives an angle of 7° in the crystal. Allowing for these depolarizing factors, the results are entirely consistent with the EQ(Γ_{25}^+)-ED Raman mechanism.

As an additional check on the consistency of the EQ(Γ_{25}^+)-ED Raman tensors, we list in Table V the

TABLE IV. Polarization study of Raman scattering in resonance with 1SY exciton for backscattering in the $x-y(\hat{\epsilon},\hat{\epsilon}')y-x$ configuration. Observed and calculated intensities are given as in Table III.

Phonon	(V,V) $(x+y,x+y)$	(V,H) $(x+y,z)$	(H,V) $(z,x+y)$	(H,H) (z,z)
$\Gamma_{25}^-(88\ \mathrm{cm}^{-1})$				
obs.	0.09	0.14	0.80	1.2
calc.	0	0	d^2	d^2
$\Gamma_{12}^-(109\ \mathrm{cm}^{-1})$				
obs.	4.1	1.7	39.0	15.1
calc.	0	0	$3b^2$	0
$\Gamma_{15}^{-(1)}$(TO: 152 cm^{-1})				
obs.	0.04	0.05	0.35	0.41
calc.	0	0	0	0
$\Gamma_{15}^{-(1)}$(LO: 154.5 cm^{-1})				
obs.	0.02	0.09	0.10	1.46
calc.	0	0	0	$(c_{D_1}+c_{F_1})^2$
$\Gamma_2^-(350\ \mathrm{cm}^{-1})$				
obs.	0.004	0.005	0.08	0.018
calc.	0	0	0	0
$\Gamma_{15}^{-(2)}$(TO: 635 cm^{-1})				
obs.	0.07	0.04	0.11	0.13
calc.	0	0	0	0
$\Gamma_{15}^{-(2)}$(LO: 665 cm^{-1})				
obs.	0.09	0.18	0.40	1.90
calc.	0	0	0	$(c_{D_2}+c_{F_2})^2$

TABLE V. Relative values of the square amplitudes of Raman constants for odd-parity phonons in terms of observed scattering from the Γ_{25}^- phonon. Determinations are made from the data of Tables III and IV.

	$\Gamma_{12}^-: b^2/d^2$	$\Gamma_{15}^{-(1)}(\mathrm{TO}): c_{D_1}^2/d^2$	$\Gamma_{15}^{-(1)}(\mathrm{LO}): (c_{D_1}+c_{F_1})^2/d^2$	$\Gamma_2^-: a^2/d^2$	$\Gamma_{15}^{-(2)}(\mathrm{TO}): c_{D_2}^2/d^2$	$\Gamma_{15}^{-(1)}(\mathrm{LO}): (c_{D_2}+c_{F_2})^2/d^2$
Table III	12.5	0.93	1.83	0.15	0.48	2.63
Table IV	13	...	1.46	...	...	1.90

ratios of Raman constants calculated from the data in Tables III and IV. The differences between the two determinations of the ratios b^2/d^2, $(c_{D_1}+c_{F_1})^2/d^2$, and $(c_{D_2}+c_{F_2})^2/d^2$ are within the typical experimental uncertainty of 30%, due mainly to the presence of significant scattering in forbidden polarizations. The ratios of the Raman constants can be related through Eq. (1) to the relative sizes of the exciton-lattice matrix element for the various phonons, $\sum_a \langle a|\mathcal{H}_{EL}^{(j,\sigma)}|b\rangle$. This can be done since only a single set of band states for the electron and hole of the virtual states $|a\rangle$ are important for each phonon. These states have been determined by Birman from the accepted band structure of Cu_2O.[14]

The angular dependence of Raman scattering on ω_i at the 1SY exciton is readily obtained from the EQ(Γ_{25}^+)-ED tensors. The predicted intensity of backscattering in the $x-y(z, x\cos\psi/\sqrt{2}+y\cos\psi/\sqrt{2}+z\sin\psi)y-x$ configuration, which corresponds to $\hat{\epsilon}'$ making an angle ψ with the $x+y$ direction is given in Table VI. The prediction for the Γ_{15}^- mode had previously been given incorrectly.[3,14] We have measured the angular dependence in this geometry, and a comparison with theory for allowed phonons is presented in Fig. 1. As we have already noted, scattering is not extinguished in forbidden polarizations, due to the imperfect optical quality of our crystal, and we have accounted for this by adding an angle-independent component to the predictions of Table VI for the Γ_{12}^- and Γ_{15}^- phonons, which is equal to the scattering intensity observed in forbidden configurations. This procedure is supported by our observation that residual scattering from the two $\Gamma_{15}^-(\mathrm{TO})$ phonons, which are forbidden in this geometry for all analyzer angles, is nearly independent of the angle ψ. With this assumption we obtain agreement with theory.

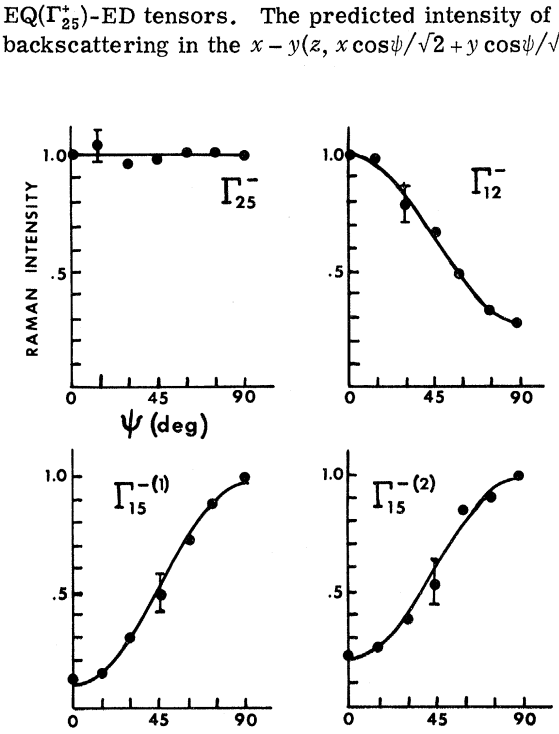

FIG. 1. Angular dependence of the normalized intensity of Raman scattering from the Γ_{25}^-, Γ_{12}^-, $\Gamma_{15}^{-(1)}(\mathrm{LO})$, and $\Gamma_{15}^{-(2)}(\mathrm{LO})$ phonons. Data were taken in a backscattering geometry from the $(1\bar{1}0)$ face of Cu_2O with the laser in resonance with the 1SY exciton; $\hat{\epsilon}$ was parallel to [001] and ϵ' formed an angle ψ with [110]. The theoretical curve is given by adding a constant, equal to the scattering observed in the forbidden orientation, to the predictions in Table VI.

III. POLAR PHONONS

In Sec. II we have given the results of Raman scattering from both polar Γ_{15}^- modes in Cu_2O. Scattering from these modes is of special interest since the LO phonon carries an electric field $\vec{E}_L$, which produces an LO-TO splitting and leads to additional scattering for the LO component. The Fröhlich interaction, associated with $\vec{E}_L$, is specific to polar LO phonons, whereas the deformation-potential interaction is presumed to be the same for both LO and TO phonons.

The Fröhlich electron-lattice interaction for LO phonons of wave vector $\vec{q}$ is given by[9]

$$V_{EL}^F(\omega_{LO}, \vec{q}, \vec{r}) = (e\gamma_{\omega_{LO}}/q)\, e^{i\vec{q}\cdot\vec{r}} = (e\gamma_{\omega_{LO}}/q)\left[1+i\vec{q}\cdot\vec{r}-\tfrac{1}{2}(\vec{q}\cdot\vec{r})^2+\cdots\right], \quad (5)$$

where e is the electronic charge and $\gamma_{\omega_{LO}}$ is pro-

TABLE VI. Predicted intensity of Raman scattering via the EQ(Γ_{25}^+) – ED mechanism for backscattering in the $x-y(z, x\cos\psi/\sqrt{2}+y\cos\psi/\sqrt{2}+z\sin\psi)y-x$ configuration. The corresponds to $\hat{\epsilon}'$ making an angle ψ with the $x+y$ direction.

	Γ_{25}^-	Γ_{12}^-	$\Gamma_{15}^-(\mathrm{TO})$	$\Gamma_{15}^-(\mathrm{LO})$	Γ_2^-
$I^j(\psi)$	d^2	$3b^2\cos^2\psi$	0	$(c_D+c_F)^2\sin^2\psi$	0

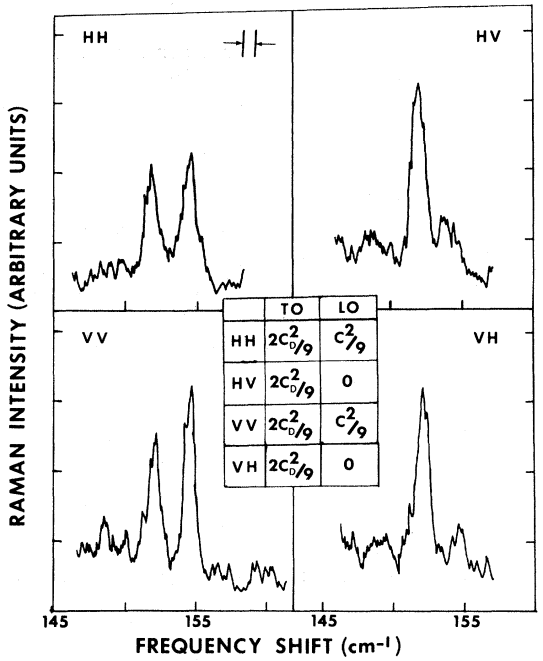

	TO	LO
HH	$2c_D^2/9$	$c_F^2/9$
HV	$2c_D^2/9$	0
VV	$2c_D^2/9$	$c_F^2/9$
VH	$2c_D^2/9$	0

FIG. 2. Raman spectra for four polarizations showing the LO and TO components of the $\Gamma_{15}^{-(1)}$ mode. The experiment was performed in a backscattering geometry from the (111) crystal face with the laser in resonance with the 1SY exciton state. All spectra are shown on the same scale with a resolution of 0.9 cm^{-1}. The inserted table gives theoretical predictions for Raman intensities as calculated from Table II; $c = c_D + c_F$. In the two configurations for which both lines were observed, the ratios of the LO to TO intensities are twice those predicted by assuming the scattering is only due to the deformation-potential interaction.

portional to $\vec{E}_L$. The monopole term in the expansion does not contribute to the exciton-lattice matrix element, since the contributions of the electron and hole cancel. The dipole term has odd parity. In crystals with inversion symmetry it cannot, therefore, contribute to ordinary ED-ED Raman scattering, but it may participate in EQ-ED scattering. Since the dipole Fröhlich interaction has the same symmetry as the deformation-potential interaction for the Γ_{15}^-(LO) phonon, the amplitude for scattering from a Γ_{15}^-(LO) phonon is the coherent sum of amplitudes for these two interactions, $c = c_D + c_F$.

In the absence of the Fröhlich interaction, the Raman constants for LO and TO scattering would be identical. The observed enhancement of the Raman constant for the LO phonon ($c_D + c_F$) relative to that for the TO phonon (c_D) is, therefore, a measure of the importance of the Fröhlich interaction at the 1SY exciton. In Table V we find $(c_{D_1} + c_{F_1})^2 \simeq 2c_{D_2}^2$ for the $\Gamma_{15}^{-(1)}$ mode and $(c_{D_2} + c_{F_2})^2 \simeq 5.5\, c_{D_2}^2$ for the $\Gamma_{15}^{-(2)}$ mode. This is consistent with the large LO-TO splitting of 30 cm^{-1} for the $\Gamma_{15}^{-(2)}$ mode, as compared to the 2.5-cm^{-1} splitting of the components of the $\Gamma_{15}^{-(1)}$ mode.

The dipole Fröhlich interaction can be the source of strong resonant enhancement of Raman scattering from LO phonons because it can couple electronic states in the same band[15] and the two denominators in Eq. (1) can thus simultaneously become small. The dipole Fröhlich term leads to resonant enhancement by coupling exciton states of opposite parity in the same exciton series. Our results are the first observation of this normally forbidden mechanism in first-order Raman scattering.

The 1SY exciton is most strongly coupled via the intraband Fröhlich interaction to P states of the yellow series. The 2PY state, which is the lowest-lying excited state, is more than 900 cm^{-1} above the 1SY exciton. This is a rather large energy separation for states within the same exciton series and leads to a relatively large energy denominator associated with the scattered photon in the expression for the cross section given in Eq. (1). Fröhlich scattering does not, therefore, dominate the first-order Raman spectrum near resonance with the 1SY exciton. For a laser frequency in resonance with one of the excited states, however, this energy denominator can become quite small, since exciton levels are more closely spaced and the contribution of the Fröhlich mechanism to Raman scattering should be increased. We have observed such a large enhancement of scattering from the $\Gamma_{15}^{-(1)}$(LO) phonon in the excited states of the yellow series. A comparison of scattering from the $\Gamma_{15}^{-(1)}$ phonons at the 1SY exciton and in the excited states with a laser frequency of 17475 cm^{-1} is presented in Figs. 2 and 3. The experiment was done in the $x+y+z\,(\hat{\epsilon}, \hat{\epsilon}') - x - y - z$ scattering orientation for which both LO and TO components are theoretically allowed in the EQ-ED approximation. In Fig. 2 the LO intensity at the 1SY state is twice that predicted on the basis of purely deformation-potential scattering. In the excited states, however, only LO scattering is observed, indicating that the scattering is entirely via the Fröhlich interaction. Details of the scattering in the excited states will be given in a subsequent publication.[16]

In previous observations of the resonant enhancement of Raman scattering from forbidden polar LO phonons in various crystals,[17] it has generally been assumed that the dominant mechanism is ED-ED Raman scattering with the quadrupole-Fröhlich-interaction term in Eq. (6) taken as the exciton-lattice interaction, a mechanism which has been discussed by Martin.[18] The quadrupole-Fröhlich interaction is linear in q, and the Raman intensity is of the form[3,19]

$$I(\mathrm{LO}) = C \left| \sum_{\alpha\beta\gamma} \epsilon'_\alpha \overline{P}_{\alpha\beta\gamma}(\mathrm{LO}) \epsilon_\beta q_\gamma \right|^2 , \qquad (7)$$

where $\overline{P}_{\alpha\beta\gamma}$(LO) is a third-rank tensor. Here q

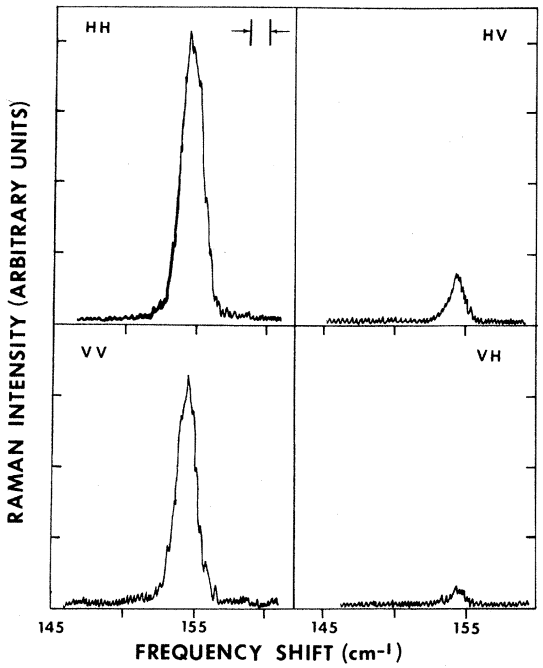

FIG. 3. Raman spectra for four polarizations of the $\Gamma_{15}^{-(1)}$ mode with $\omega_i = 17\,475$ near the $n=4$ exciton state of the yellow series. All spectra are shown on the same scale with a resolution of 1.2 cm. Only the LO component is observed, indicating the importance of the Fröhlich interaction here.

plays a role similar to k for EQ-ED scattering. This mechanism was first proposed by Martin and Damen[18,20] to explain the observation of forbidden scattering from LO phonons in CdS. By comparison, the intensity of Raman scattering in the EQ-ED mechanism via the dipole-Fröhlich interaction is given by Eq. (4) with $j\sigma = \Gamma_{15}^{-}(\mathrm{LO})$.

Forbidden Raman scattering from LO phonons in Cu_2O has previously been observed by Williams and Porto.[15,21] Their observations were made with the laser frequency in the range of the blue exciton series, and they have explained their results by the Martin mechanism. In Sec. V we will discuss how one can distinguish the EQ-ED Raman mechanism via the dipole Fröhlich interaction from the Martin mechanism, which involves the quadrupole Fröhlich interaction.

IV. EXPERIMENTAL TEST OF RAMAN-TENSOR SYMMETRY

In the usual ED-ED Raman scattering, the exciton-radiation coupling is identical for the incident and scattered photon and the Raman tensor is, therefore, automatically symmetric with respect to interchange of the incident and scattered polarizations.[6] On the other hand, the polarization-selection rules for the EQ-ED mechanism are asymmetric, as a result of the quadrupole-exciton-radiation coupling, and this allows us to unambiguously test a number of underlying symmetries which all Raman tensors must possess. We have tested the invariance of the EQ(Γ_{25}^{+})-ED Raman tensor under time reversal and the relation of the scattering amplitudes for "in" and "out" resonances—processes in which either the incident or scattered radiation is resonant with the 1SY exciton. In the limit that the phonon frequency is negligible compared to the energy difference between the electronic states involved, the scattering amplitudes for "in" or "out" resonances should be equal.[6] These symmetry relations can be shown to hold from Eq. (1). The asymmetry of the EQ-ED mechanism allows the possibility, which is realized in our experiments, of a particular Raman-scattering process being allowed in a single combination of incident and scattered polarizations. The scattering configuration for the symmetry-related process is, consequently, uniquely specified with the incident and scattered polarizations interchanged.

We have performed resonant-Raman experiments at the 1SY exciton at 80 °K. We measured scattering from the Γ_{12}^{-} phonon with appropriate polarizations to check the symmetries mentioned above. The Γ_{12}^{-} phonon couples the 1SY level to S states of the blue exciton series with energies $\hbar\omega_{nSB}$.[14] Since the ratio of the energy difference between the coupled exciton states to the Γ_{12}^{-} phonon frequency is large, $[(\omega_{nSB} - \omega_{1SY}/\omega_0] \approx 35$, the ratio of scattered intensity for "in" and "out" resonances should be close to unity.

The allowed polarizations for Raman scattering for the four cases we considered are shown in Fig. 4. We note that for processes related by a single symmetry relation, the polarizations in and out of the scattering plane of the incoming and scattered wave are reversed. The time-reversed process of the "in"-resonance Stokes scattering in Fig. 4(a) is one with all photon and phonon-propagation vectors reversed and with all polarizations unchanged as shown in Fig. 4(a). For experimental convenience, however, the incident wave vector was always kept along the $+x$ direction. The anti-Stokes "out" resonance in Fig. 4(c) is related to the process of Fig. 4(b) by a rotation of π around the $x+y$ direction. Since a cubic crystal is invariant under this rotation (C_2), we may loosely consider Figs. 4(a) and 4(c) to be related by time reversal, or more precisely by the operation TC_2. The processes shown in Figs. 4(d) and 4(f) are similarly related through TC_2.

In our measurements of polarized scattering for the processes shown in Fig. 4, we find the intensites in allowed polarizations are at least a factor of 10 larger than in forbidden polarizations. In addition to verifying the polarization predictions,

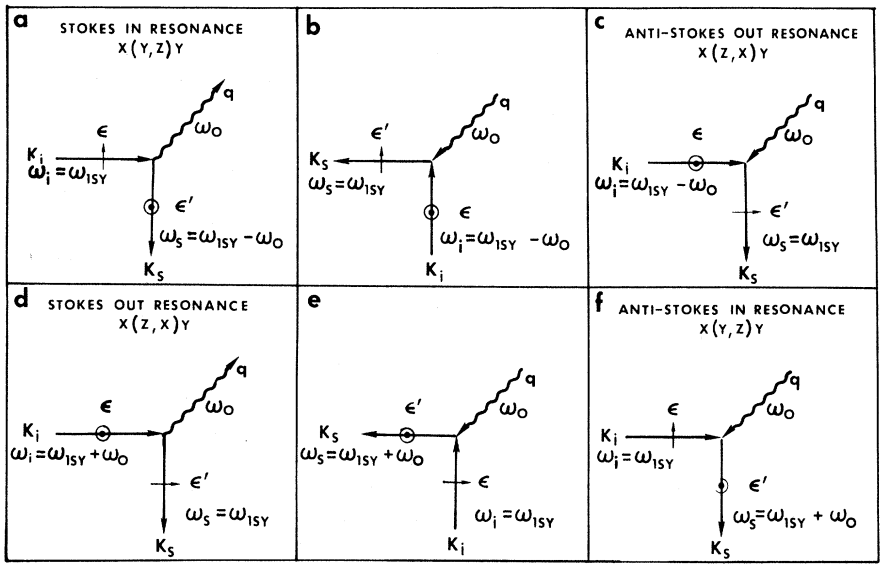

FIG. 4. Diagramatic representation of related processes involving resonant scattering at the 1SY exciton state from a Γ_{12}^{-} phonon. Actual experiments were performed in configurations represented in (a), (c), (d), and (f). Processes represented in (b) and (e) are the time-reversed processes of (a) and (d). The straight lines represent photons whose frequencies are given in the diagram, and the wavy lines represent phonons with frequency $\omega_0 = 109\ \mathrm{cm}^{-1}$.

which are determined by symmetry, we have compared the observed ratio of intensities in allowed configurations to theory. The time reversal of Stokes scattering is an anti-Stokes process. Though the Raman tensors for these processes have the same magnitude by symmetry, the Stokes scattering should be more intense by the ratio $(n+1)/n$, where n is the Bose factor for the phonon. At 80 °K this ratio is 7.1 for the 109-cm^{-1} phonon.

In the experiment the laser beam traverses a 1-mm-thick crystal very close to the edge that faces the collecting optics. The observed intensity of the Raman light was corrected for the absorption of the laser beam along the 1-mm path but not for the absorption of the scattered light, since the distance of the beam from the crystal edge was small and not precisely known. We estimate this leads to an uncertainty of less than 3% in the Raman cross section. The ratios of the Raman intensities corrected for absorption are given in Table VII. They are in agreement with theory within the margin of experimental uncertainty of 10%, which is due primarily to an uncertainty of ±2 °K in the crystal temperature.

Next we consider the symmetry between "in" and "out" resonances by examining the resonant matrix elements in Eq. (1) for these processes. For Stokes scattering, at an "in" resonance at the 1SY exciton, the resonant matrix element for the Raman amplitude is given by taking $\omega_i - \omega_{1SY} = i\Gamma_{1SY}$ and $|b\rangle = |1\mathrm{SY}\rangle$, while at an "out" resonance we take $\omega_i - \omega_{1SY} - \omega_0 = i\Gamma_{1SY}$ and $|a\rangle = |1\mathrm{SY}\rangle$. For scattering along the principal axes, the Raman tensors for these processes shown in Figs. 4(a) and 4(d) are the transpose of one another with regard to the incident- and scattered-light polarizations, aside from a small discrepancy in the nonresonant factor in the denominator. The same holds for the "in" and "out" anti-Stokes processes shown in Figs. 4(d) and 4(c).

The Γ_{12}^{-} phonon couples the 1SY exciton to S states of the blue series. The nonresonant factor in the denominator of the transition matrix element in Eq. (1) with the nS level of the blue series taken as an intermediate state is $(\omega_{1SY} - \omega_{nSB} - \omega_0)$ for an "in" resonance and $(\omega_{1SY} - \omega_{nSB} + \omega_0)$ for an "out" resonance. Wu and Birman calculated the intensity ratio between an "in" and "out" resonance by summing over all intermediate states. The essentials of such a calculation are described elsewhere.[5] Using positions for the states of the blue series determined from absorption[22] and reflection[21] data at 80 °K, the ratio of the scattering amplitudes of an "in" and "out" resonance is 0.91. This is close to the value one would obtain by considering only the coupling to the 1S blue level. The ratios for both Stokes and anti-Stokes processes corrected for the effects of absorption are given in Table VII

TABLE VII. Ratios of intensities of Raman scattering, corrected for absorption, for the four processes shown in (a), (b), (c), and (d) of Fig. 4. Experiment performed at 80° ± 2 °K. Temperature uncertainty leads to uncertainty in theoretical ratio of scattering for time-reversed processes.

Experiment	Theory
Ratios for time-reversed processes	
$I(a)/I(c) = 6.6 \pm 0.4$	7.1 ± 0.6
$I(d)/I(f) = 7.2 \pm 0.4$	
Ratios for "in" and "out" resonances	
$I(a)/I(d) = 0.96 \pm 0.05$	0.91
$I(f)/I(c) = 0.95 \pm 0.05$	

and agree with theory within experimental uncertainty. Thus we find that observed polarizations and relative intensities of Raman scattering at the 1SY exciton are in agreement with the expected symmetry of the Raman tensor.

V. CONCLUSION

We have described many of the unique features of EQ-ED resonance Raman scattering. This new type of scattering is complementary to the usual allowed Raman scattering. Important features of the effect are the activation of forbidden phonons and the dependence of scattering upon the wave vector of the incident (scattered) radiaton at an "in" ("out") resonance with a dipole-forbidden state. Our experimental study of polarized scattering from odd-parity phonons at the 1SY level of Cu_2O agrees with the predictions of the third-rank tensors derived by Birman for the EQ-ED mechanism. The agreement with these tensors for different scattering geometries is additional confirmation of the dependence of the scattering upon the propagation direction of the photon wave vector. We have taken advantage of the fact that the scattering tensor is asymmetric to demonstrate explicitly the symmetry of the Raman tensor under time reversal and the relationship of scattering at an "in" and "out" resonance.

From a comparison of the intensities of the LO and TO components of the two polar modes, which we have fully resolved for the first time, the contribution of the Fröhlich interaction to scattering at the 1SY exciton is estimated. The enhanced scattering is due to dipole Fröhlich coupling between the 1SY exciton and P states of the yellow series. The values of ω_{LO} and ω_{TO} obtained for the two polar modes can be used to estimate the static-dielectric constant from the measured value of ϵ_∞.[23] From the generalized Lyddane-Sachs-Teller relation,[24] $\Pi_{\sigma=1}^2(\omega_{LO}^\sigma/\omega_{TO}^\sigma)^2 = \epsilon_0/\epsilon_\infty$, we obtain a value of 7.33 for ϵ_0.

Previous observations of forbidden Raman scattering from LO phonons in many crystals have been explained by the mechanism proposed by Martin[18] of ED-ED scattering via the quadrupole Fröhlich interaction. The possibility that the EQ-ED mechanism is involved in previously observed resonant enhancement of Raman scattering from LO phonons should be explored further.

The ratio of scattering intensity of EQ-ED Raman scattering via the dipole Fröhlich interaction to scattering via the Martin mechanism is of order $(k/q)^2$. Except for small-angle scattering, when scattering via the Martin mechanism vanishes or is small, these two mechanisms could give rise to first-order scattering with comparble scattering cross sections. In second-order Raman scattering, q is unrestricted and the two mechanisms could be distinguished by the relative intensity of first- and second-order scattering.[25] In addition, there are three primary features that can differentiate between the EQ-ED mechanism and the Martin mechanism in first-order Raman scattering. They are the polarization of scattering, the frequency of peak resonance enhancements, and the dependence of scattering on the magnitude of the phonon wave vector $\vec{q}$ in the Martin mechanism. The Raman tensor is expected to be diagonal for the Martin mechanism for isotropic excitons,[18] whereas off-diagonal scattering may occur in some crystal orientations for the EQ-ED mechanism. For the EQ-ED mechanism, the frequency of maximum enhancement depends on the positions of dipole-forbidden levels, as well as of allowed levels. This can be checked most readily in a crystal such as Cu_2O which has well-defined excitonic structure. Finally, a comparison of scattering in the forward and backward direction could settle the question of the q dependence of the Raman cross section. Colwell and Klein[26] carried out such an experiment in CdS and found the Raman cross section to be independent of scattering angle. However, the broad phonon line and large cross section they observed indicated that scattering was not due to a forbidden intrinsic mechanism but to localized excitons.[27] Of course, in some cases, the Martin mechanism and the EQ-ED Fröhlich mechanism may both contribute to resonant Raman scattering.

ACKNOWLEDGMENTS

We are indebted to J. L. Birman, R. A. Forman, and C. H. Wu for many valuable discussions during the course of this work. We would also like to thank R. A. Forman, W. S. Brower, Jr., and H. S. Parker for providing the crystals for this experiment.

[1] A. Compaan and H. Z. Cummins, Phys. Rev. Lett. 31, 41 (1973).
[2] E. F. Gross and A. A. Kaplyanski, Fiz. Tverd. Tela. 2, 379 (1960) [Sov. Phys.-Solid State 2, 353 (1960)]; S. Nikitine, J. B. Green, and M. Gertier, Phys. Kondens. Materie 1, 214 (1963).
[3] J. L. Birman, Phys. Rev. B 9, 4518 (1974).
[4] J. L. Birman, *Theory of Crystal Space Groups and Infra-Red and Raman Processes in Insulating Crystals*, in *Handbuch der Physik*, edited by S. Flügge (Springer, New York, 1974), Vol. 25.
[5] C. H. Wu and J. L. Birman, Solid State Commun. 13, 1189 (1973).
[6] R. Loudon, Proc. R. Soc. Lond. A 275, 218 (1963).
[7] R. Loudon, Adv. Phys. 13, 423 (1964).
[8] H. Poulet, Ann. Phys. (N.Y.) 10, 908 (1955).
[9] H. Fröhlich, Adv. Phys. 3, 325 (1954).
[10] A. Z. Genack (unpublished).

[11]W. S. Brower Jr. and H. S. Parker, J. Crystal Growth 8, 227 (1971).
[12]Air Products and Chemicals Inc., Allentown, Pa.
[13]A. Compaan and H. Z. Cummins, Phys. Rev. B 6, 4753 (1972).
[14]J. L. Birman, Solid State Commun. 13, 1189 (1973).
[15]P. F. Williams, Ph.D. thesis (University of Southern California, 1973) (unpublished).
[16]A. Z. Genack, M. A. Washington, A. Compaan, and H. Z. Cummins (unpublished).
[17]See, for example, *Light Scattering in Solids*, edited by M. Balkanski (Flammarion, Paris, 1971), Chap. 2.
[18]R. M. Martin, Phys. Rev. B 4, 3676 (1971).
[19]R. M. Martin, in *Light Scattering in Solids*, edited by M. Balkanski (Flammarion, Paris, 1971), p. 25.
[20]R. M. Martin and T. C. Damen, Phys. Rev. Lett. 26, 86 (1971).
[21]P. F. Williams and S. P. S. Porto, Phys. Rev. B 8, 1782 (1972).
[22]S. Daunois, J. L. Deiss, and B. Meyer, J. Phys. 27, 142 (1966).
[23]M. O'Keefe, J. Chem. Phys. 39, 1789 (1963).
[24]W. Cochran and R. A. Cowley, J. Phys. Chem. Solids 23, 447 (1962).
[25]E. F. Gross, S. A. Permogorov, V. V. Tranikov, and A. V. Sel'kin, in *Light Scattering in Solids*, edited by M. Balkanski (Flammarion, Paris, 1971), p. 238.
[26]P. J. Colwell and M. V. Klein, Solid State Commun. 8, 2095 (1970).
[27]Recently, Permogorov has observed a 30% asymmetry in an experiment similar to Colwell and Klein's, using an extremely high-purity CdS sample [S. A. Permagorov (private communication)].